CO oxidation on Pt(111) at near ambient pressures

S. Krick Calderón, M. Grabau, L. Óvári, B. Kress, H.-P. Steinrück, and C. Papp

Citation: The Journal of Chemical Physics **144**, 044706 (2016); doi: 10.1063/1.4940318
View online: http://dx.doi.org/10.1063/1.4940318
View Table of Contents: http://scitation.aip.org/content/aip/journal/jcp/144/4?ver=pdfcov
Published by the AIP Publishing

CO oxidation on Pt(111) at near ambient pressures

S. Krick Calderón,[1] M. Grabau,[1] L. Óvári,[2] B. Kress,[1] H.-P. Steinrück,[1,3] and C. Papp[1]
[1]*Lehrstuhl für Physikalische Chemie II, Universität Erlangen-Nürnberg, Egerlandstr. 3, 91058 Erlangen, Germany*
[2]*MTA-SZTE Reaction Kinetics and Surface Chemistry Research Group, Rerrich Béla tér 1, 6720 Szeged, Hungary*
[3]*Erlangen Catalysis Resource Center, Egerlandstr. 3, 91058 Erlangen, Germany*

(Received 18 October 2015; accepted 8 January 2016; published online 27 January 2016)

The oxidation of CO on Pt(111) was investigated simultaneously by near ambient pressure X-ray photoelectron spectroscopy and online gas analysis. Different CO:O_2 reaction mixtures at total pressures of up to 1 mbar were used in continuous flow mode to obtain an understanding of the surface chemistry. By temperature-programmed and by isothermal measurements, the onset temperature of the reaction was determined for the different reactant mixtures. Highest turnover frequencies were found for the stoichiometric mixture. At elevated temperatures, the reaction becomes diffusion-limited in both temperature-programmed and isothermal measurements. In the highly active regime, no adsorbates were detected on the surface; it is therefore concluded that the catalyst surface is in a metallic state, within the detection limits of the experiment, under the applied conditions. Minor bulk impurities such as silicon were observed to influence the reaction up to total inhibition by formation of non-platinum oxides. © *2016 AIP Publishing LLC.* [http://dx.doi.org/10.1063/1.4940318]

I. INTRODUCTION

X-ray Photoelectron Spectroscopy (XPS) is one of the most widely used techniques regarding the investigation of surface reactions.[1–5] Its surface sensitivity results from the limited mean free path of the photoelectrons in condensed matter, which restricts the information depth to the topmost layers of a sample. At the same time, the interaction of the photoelectron with atoms and molecules in the gas phase also represents one major drawback in conventional photoelectron spectroscopy for studying surface reactions, since for this reason conventional setups require ultrahigh vacuum (UHV) conditions; in other words, the pressure range of the gases applied during XPS is limited to pressures typically below 10^{-6} mbar.[1,6] With the aim of surface science to provide a fundamental basis for the optimization of catalysts and a molecular understanding of the relevant reaction steps, the difference between these low pressures and the actual reaction conditions of real catalysts needs to be considered. The term "pressure gap"[7–9] describes the contrast between the pressure ranges used in real and model catalysis studies and indicates that results obtained in surface science often cannot be simply extrapolated to higher pressures.[10] To narrow or even close this gap, different established surface science techniques such as XPS[7,11,12] and Scanning Tunneling Microscopy (STM)[13] have been refined towards the use at higher pressures, often denoted as near ambient pressure (NAP) conditions. As this is a new and evolving field of surface science, there is the need to carefully probe even well-understood model reactions at these quite different conditions. Compared to a classical surface science experiment in UHV, entirely new effects have to be considered. One example is the occurrence of strong heat and mass transfer effects[14–16] that have been reported for reactions on transition metals, such that the reaction kinetics at elevated pressures are drastically influenced by the diffusion of reactants and products. These effects were, e.g., observed for CO oxidation on Pd and RuO_2,[14,15] which are both well investigated and understood model reactions under surface science conditions.

On Pt(111), CO oxidation under UHV conditions follows a Langmuir-Hinshelwood mechanism, that is, both reactants have to be adsorbed as next neighbours on the surface in order to react.[17,18] The activation energy of this reaction strongly depends on the oxygen and carbon monoxide coverages: under CO rich conditions, the surface is poisoned as oxygen cannot adsorb and dissociate, which is required for the reaction to occur.[19–21] Interesting effects like an oscillatory behaviour[22] of this reaction have been reported to take place under UHV conditions[23,24] and also at ambient pressures.[25] While the oscillations for Pt(100) observed in UHV[23,24] are induced by surface phase transitions, at high pressures this behaviour was attributed to SiO_2 formation due to platinum bulk impurities.[25] In the last years, an intense debate arouse[13,26–28] with respect to CO oxidation at higher pressures, especially concerning the state of the catalyst in the active range. Whereas Hendriksen *et al.*[13,29,30] suggested a Mars-van Krevelen oxidation-reduction mechanism for Pt(110) and also Pd(100), with the respective metal oxide as highly active species, other groups report a metallic state of the surface in the most active regime.[26] As techniques like STM, Sum Frequency Generation (SFG), and Infrared Spectroscopy (IR), which were used in other studies,[16,29,31] lack direct chemical information on the oxidation state of the surface or the quantification of adsorbates, NAP-XPS could step in as a powerful quantitative tool. Indeed, the formation of platinum oxide above a certain oxygen pressure and at elevated temperatures has been reported before,[16,32] with these oxides

being reducible by exposure to H_2.[33] Nevertheless, it still has to be examined whether platinum oxide also exists under reaction conditions and if it actively takes part in the reaction, i.e., it is reactive towards CO.

Herein, we report on *in situ* NAP-XPS results of the CO oxidation on Pt(111). The CO oxidation reaction was also monitored by online gas analysis using a quadrupole mass spectrometer (QMS). We deduce that the reactive state of the platinum surface during CO oxidation is metallic and that no detectable amounts of platinum oxide are present under the applied reaction conditions of up to 1 mbar. We also report on poisoning of the surface by CO and "non-platinum"-oxides resulting from bulk impurities of the crystal.

II. EXPERIMENTAL DETAILS

The Pt(111) crystals were cleaned by cycles of Ar^+ sputtering at 1×10^{-5} mbar (1 kV, room temperature, 20 min, I_{sample} = 5–12 μA) and annealing at 1100 K (3 min). The cleanness of the sample was checked by XPS and surface order of the clean surface was verified by LEED. The purity of the Pt(111) crystals was 99.999% and an accuracy of the polishing angle of <0.1° was denoted by the supplier (MaTecK). The purity of the used gases was 4.7 for CO and 5.0 for O_2.

The detailed setup of the NAP-XPS chamber has been described elsewhere.[34] Shortly, it consists of an electron energy analyser (modified Omicron EA-125) that is separated by four differential pumping stages from the reaction area at near ambient pressures, enabling collection of XP spectra at 1 mbar while maintaining high vacuum in the analyser. As excitation source, a modified Al/Mg dual anode (Specs XR-50 HP) was used. All spectra in this work were taken at normal emission with Mg K_α radiation (1253.6 eV) except for the slow heating ramp of the 1:10 CO:O_2 mixture which was taken with Al K_α radiation (1486.6 eV). The UHV environment of the X-ray gun is sealed against the high pressures within the measurement chamber by a 200 nm thick Si_3N_4 window. A base pressure in the range of 10^{-9} mbar allows UHV experiments in addition to the near ambient pressure investigations. Exposure to reactive gases was achieved by background dosing through two separate leak valves; a MKS Barathron 121A pressure gauge (10^{-4}–1 mbar) was used to ensure gas type independent pressure measurement. The sample was heated by resistive heating, and the temperature was measured using a chromel-alumel thermocouple directly spot-welded to the crystal.

Region scans of the Pt 4f, O 1s, and C 1s core levels as well as wide scans were taken to monitor the reaction *in situ* and also to describe the surface before and after the reaction. The binding energies of the O 1s region were referenced to the CO bridge and on-top binding energies (531.1 and 532.8 eV, respectively),[35] whereas the Pt 4f spectra were referenced to the Fermi edge. The acquisition time for the O 1s region during the CO oxidation reaction was ~5 min for the isothermal reactions, ~2 min for the heating ramps with 2 K/s and 1 K/s), and ~8 min for the heating ramp with 2 K/min in the temperature-programmed measurements. Please see Table S1 of the supplementary material[36] for details on the fitting procedure. All coverages given were obtained with an accuracy of approximately ±0.15 ML, obtained from a comparison to the well-known c(2 × 4) CO superstructure with a coverage of 0.5 ML.[37] Thereby, 1 ML corresponds to one adsorbate molecule or atom per surface atom on the Pt(111) surface.

A quadrupole mass spectrometer (Prisma QMS 200, Pfeiffer Vacuum) is attached to the second differentially pumped stage, allowing simultaneous online gas analysis during reaction using the Faraday cup as detector. The QM spectra were corrected for contributions due to CO_2 decomposition at the QMS filament, the different QMS sensitivities, and gas-dependent pumping of the differential pumping system.

All conversions given were calculated as $1 - (CO/CO_0) = CO_2/(CO_0)$ in percentage and to correct for changes in pressure during the experiment, CO_0 is calculated at time t as $CO(t) + CO_2(t)$.

Turnover frequencies (TOFs) were calculated from the conversions determined by online gas analysis using the method described in Ref. 38. The flux of CO molecules on the surface was calculated from the impingement rate of CO at the given partial pressure (determined from online gas analysis or calculated from XP gas phase signals) and a gas temperature of 300 K divided by the surface atom density of the Pt(111) surface (1.5×10^{15} cm^{-2}). The flux was then multiplied with the CO conversion to obtain the TOF. An error bar of ±11% for the conversions was calculated from several identical measurements.

III. RESULTS AND DISCUSSION

A. Temperature-programmed measurements

We first discuss temperature-programmed measurements, as they provide a good overview of the reaction and the occurring chemical species on the surface. The reaction was monitored by NAP-XPS and by online gas analysis using the QMS, while exposing the Pt(111) sample to a defined mixture of CO:O_2, and subsequent heating with a defined heating ramp. Figure 1(a) shows the O 1s region for the 2:1 CO:O_2 mixture. The experiment started by admitting CO to the chamber with a pressure of 0.66 mbar and the sample at 300 K. This leads to a gas phase peak at 536.6 eV and to two peaks at ~532.8 and ~531.1 eV due to CO adsorbed in on-top sites (pink) and in bridge sites (purple) on the Pt(111) surface.[20,35,39] Please note that due to the limited resolution of our setup, these two peaks are not well resolved. In Figure 1(b), exemplary fits are shown, where three successively measured O 1s spectra were added up in order to get a better signal-to-noise ratio.

At 540 s (XP spectrum 4), 0.33 mbar O_2 was added, with the sample still at 300 K, leading to an additional gas phase peak at 537.5 eV (see Figure 1(b) spectra 7-9), which consists of the two unresolved molecular O_2 gas phase signals.[40] As we first introduced CO to the chamber, the surface is blocked with CO and no adsorption of oxygen is found. From the lack of a CO_2 signal in the online gas analysis (Figure 2(b)) and the fact that no change of the adsorbate coverages is observed (Figure 1(b)) during CO and O_2 coexposure, we deduce that no reaction occurs at 300 K. The decrease of intensity of the adsorbed CO in the XP spectra by ~31% upon O_2 admission

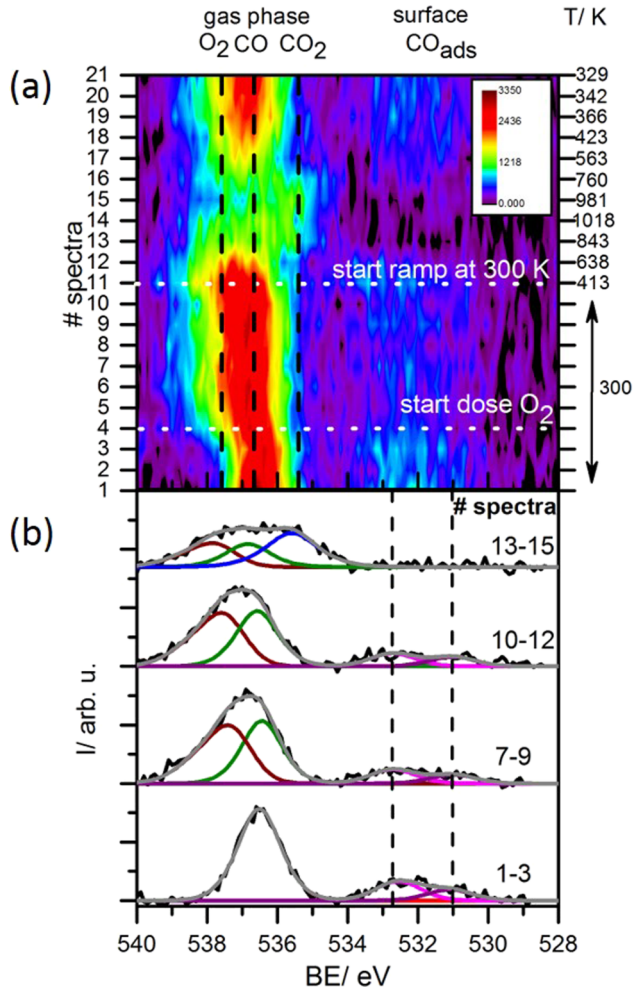

FIG. 1. O 1s region of a TPXPS experiment of the reaction of a 2:1 CO:O_2 mixture with a heating ramp 300-1100-300 K with ß = 2 K/s. (a) Colour-coded density plot of the full experiment; for details see text. (b) Selected XP spectra with the corresponding fits; note that the shown spectra are the sum of 3 neighbouring spectra to improve the signal-to-noise ratio.

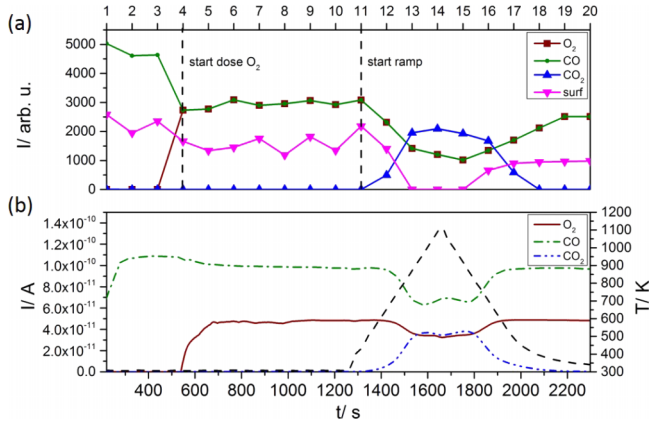

FIG. 2. Comparison of TPXPS (a) and online gas analysis (b) of the 2:1 CO:O_2 mixture with a heating ramp of ß = 2 K/s for the temperature range 300-1100-300 K.

is due to increased damping by the gas phase, whereas the loss in signal intensity resulting from the gas phase is due to partial heating of the gas phase (especially observed in spectra 13-15) by the sample and to a minor degree from changes in the sample position relative to the analyser entrance, thereby reducing the gas amount sampled by XPS. Please note that in our analysis, we use only relative amounts; therefore, this change in absolute intensity has no influence on the presented results. In the quantitative analysis of the XP spectra, shown in Figure 2(b), we used identical O 1s intensities of the gas phase for O_2 (brown squares) and CO (green circles) as constraint; this follows from the mixture of 0.66 mbar CO and 0.33 mbar O_2 and simplifies peak fitting. At 1250 s (XP spectrum 11), a heating ramp with 2 K/s was started, while XP spectra and the gas analysis were further recorded continuously. The temperature is shown as dashed line in Figure 2(b), with the temperature scale at the right axis of the figure.

At ~620 K, the onset of CO_2 production is observed by the emergence of the CO_2 signal (m/z = 44) in the online gas analysis and the respective O 1s peak of gas phase CO_2 at 535.7 eV in the XP spectra. At the same time, we also find a decrease of the reactants CO and O_2 in the gas analysis and in the XP spectra. The onset temperatures determined from XPS (Figure 2(a)) and online gas analysis (Figure 2(b)) are in a reasonably good agreement; one should note, however, that the temperature resolution of the online gas analysis is much higher than that of XPS: for the applied heating rate of 2 K/s, the online gas analysis averages over 8 K (~4 s/data point), whereas in XPS, a temperature interval of ~240 K is averaged (~2 min/spectrum). Accordingly, we use the online gas analysis for the determination of the onset temperature, which we define as the temperature, at which 10% of the maximum CO_2 production is reached. The corresponding analysis of the data in Figure 2(b) yields 620 K. Interestingly, we do not detect any adsorbed O-containing species during reaction in the XP spectra; therefore, we conclude that no (or only a minor amount of) oxide is present and that the reactive surface is in a metallic state. This is also observed in Fig. 1(b) where the XP spectra 13-15 are added up: no surface species is observed in this very reactive region, whereas CO_2 production is observed in the fits of the gas phase signals and the gas analysis. After heating the surface to 1100 K, the heating ramp was reversed, and the sample was cooled with a rate of 2 K/s. The reaction persists down to temperatures of ~420 K (10% of maximum CO_2 production). At this temperature, the O 1s peak of adsorbed CO grows again and the CO_2 gas phase signal decreases while the CO and O_2 signals rise. The same behaviour is also observed in the online gas analysis, which shows a decrease of CO_2 and an increase of CO and O_2 to the initial amounts. The observed reaction behaviour is explained by the Langmuir-Hinshelwood mechanism of the CO oxidation reaction: carbon monoxide and oxygen need to be adsorbed as next neighbours on the surface in order to react. As we chose a CO precovered surface as starting point for our experiments, some CO first needs to desorb in order to allow oxygen to be adsorbed, which is required for the reaction. This saturated CO covered surface is well-known as CO poisoned surface in the literature,[19,31] which inhibits the reaction. Note that we did not find carbon impurities on the surface after the reaction. In order to exclude influence of the X-rays on the reaction, an experiment without X-ray irradiation is compared to an experiment under X-ray irradiation; no

significant differences were observed (cf. Figure S1 in the supplementary material).[36]

When analysing the reaction behaviour, we observe a temperature difference in the QMS data between the reaction onset during heating and the termination of the reaction during cooling (see Figure S2 in the supplementary material).[36] This difference is much larger than expected from the different CO coverages on the surface that result from heating a saturated CO layer to a certain temperature or cooling the sample in a CO atmosphere to the same temperature. It is rather attributed to additional diffusion limitations (due to the finite pumping speeds) in the gas phase that are known for near ambient pressure systems: while the onset of CO_2 production is immediately monitored by XPS and online gas analysis (it occurs directly in the detection volume in front of the sample), at the end of the reaction, CO_2 from the complete reaction chamber has to be pumped away, which proceeds at a much longer time constant. This interpretation is in line with the observation that the hysteresis of the CO_2 production is significantly reduced for a slower heating ramp (hysteresis of ~33 K at 50% of the CO_2 production for a heating ramp of 1 K/s compared to ~97 K at 2 K/s for the 2:1/CO:O_2 mixture (see Figure S2 of the supplementary material)).[36]

To study the influence of the relative CO and oxygen pressures, the same type of experiment as in Figure 1 was performed for three different mixtures CO:O_2/1:1, 2:1 (stoichiometric), and 1:4, at a total pressure of 1 and 0.1 mbar. The temperature was ramped from 300 to 900 K with a heating rate of 1 K/s (averaging over 120 K in XPS). The onset temperatures are again derived from the more precise online gas analysis (10% of maximum CO_2 QMS signal). In Figures 3(a) and 3(c), they are shown as function of the oxygen concentration in the reaction mixture for total pressures of 1 and 0.1 mbar.

We find a shift to lower onset temperatures with increasing oxygen concentration. This is attributed to the fact that the reaction only sets in when CO desorption from the CO poisoned surface takes place. The lower onset temperature for higher oxygen ratios at a total given pressure is due to the higher impingement and therefore adsorption rate of oxygen, which is in competition with (re-)adsorption of CO. At a total given pressure of either 1 or 0.1 mbar, upon decreasing the CO partial pressure, the oxygen partial pressure is increased. Due to lower CO impingement rate, CO desorption sets in earlier and in addition, the increased partial pressure of oxygen promotes oxygen adsorption. At 0.1 mbar, reaction sets in at lower temperature than at 1 mbar, which is solely due to the lower CO partial pressure. Interestingly, we do not find any oxygen on the surface in the XP spectra during the reaction, thereby also ruling out the formation of a platinum oxide species. This leads to the conclusion that the reaction of adsorbed oxygen with CO as well as CO_2 desorption is fast, leading to an adsorbate free surface under the conditions investigated here.

Figures 3(b) and 3(d) show TOFs for the different mixtures as a function of temperature, as derived from the online gas analysis data. In general, the quantitative analysis from these data is, however, somewhat delicate as the results obtained from the gas analysis strongly dependent on the sample position in front of the analyser entrance, due to the concentration gradient over the surface resulting from the mass transfer limitation (MTL);[14,15,41] this is schematically illustrated in Figure 4. Therefore, for these measurements, the sample was moved to the bottom of the measurement chamber

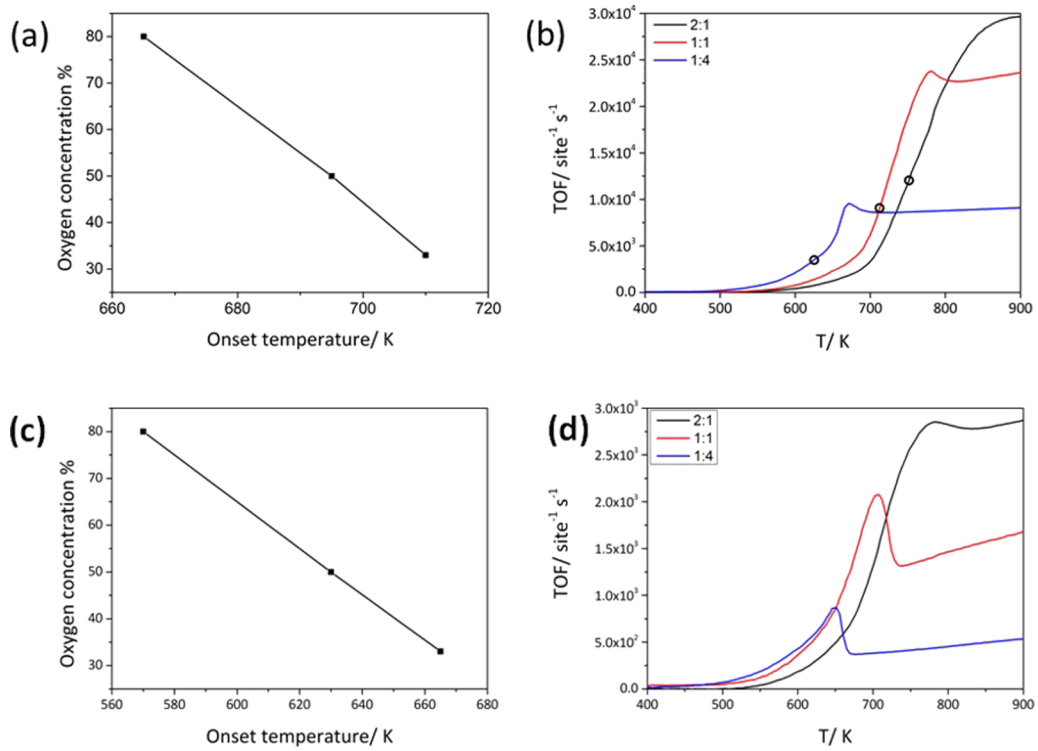

FIG. 3. (a) Onset temperature for the reaction vs oxygen concentration in the gas mixture for the online gas analysis measurements; (b) TOFs for the different CO:O_2 gas mixtures with p_{tot} = 1 mbar; (c) onset temperatures; and (d) TOFs with p_{tot} = 0.1 mbar. For further details see text.

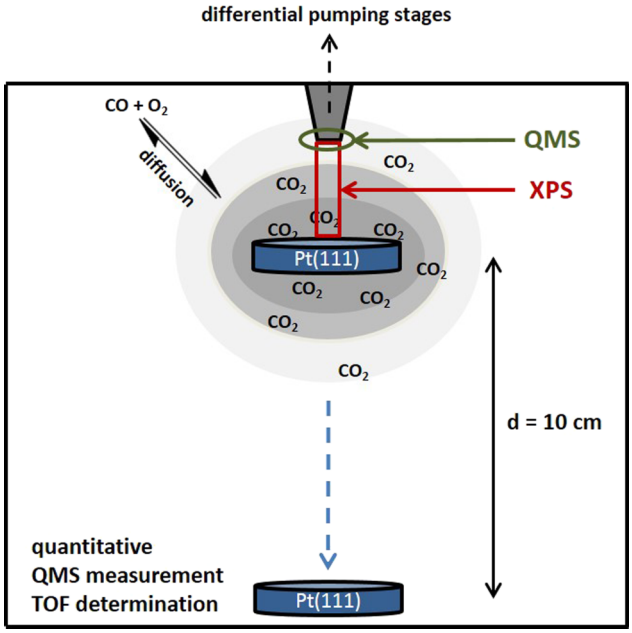

FIG. 4. Schematic drawing of the measurement chamber and gas concentration above the surface.

(d = 10 cm) where the influence of the pumping stages and the impact of an exact sample position is as low as possible (see Figure 4).

As a general trend, the temperature for reaching saturation decreases with oxygen content. Saturation indicates the point where the reaction is completely mass transfer controlled. In this regime, at a certain temperature, CO oxidation is so fast that the effective reaction rate and therefore activity are merely dependent on the diffusion of CO and O_2 to the catalyst surface; this behavior results from the build-up of a concentration gradient due to insufficient mixing of the gas phase, as depicted in Figure 4. Diffusion-controlled reaction behaviour has been reported before for similar systems such as Pt(110),[26] RuO_2,[14] and Pd.[15] Unfortunately, this effect is influencing the reaction in such manner that a more detailed analysis of the reaction kinetics is not possible in our case. The respective CO conversions are shown in Fig. S3 in the supplementary material.[36]

The highest TOFs are observed for the 2:1 $CO:O_2$ mixture, whereas the lowest maximum TOF is found for a mixture of 1:4. The high values are in general explained by the CO_2 enrichment due to insufficient mixing. Comparing the calculated TOFs to literature,[26,38] TOFs in between 10^2-10^3 s^{-1} $site^{-1}$ are found under similar conditions for Pt and Rh; also in these cases, MTLs determine the reaction and therefore the observed differences are explained by the different setups used. We observe a maximum in TOF before reaching the MTL regime for the oxidising mixtures only (1:1 and 1:4/$CO:O_2$). The same behaviour was observed before, e.g., for Pt(110) and Rh(111), and was attributed to a sudden depletion of CO in the surface-near region; it was speculated that it is connected to the presence of chemisorbed oxygen on the surface for oxidising mixtures.[26,38,42] As we did not observe any adsorbed species at this point, in our case, latter assumption is not confirmed. The fact that we observed the maximum for the oxidising mixtures exclusively is explained by the excess of oxygen (CO/O_2 = 1:4 and 1:1) for both oxidising mixtures in contrast to the stoichiometric mixture (2:1), where no such maximum occurs. Notably, in differential reactors, the conversion is usually kept at 5%-20% in order to prevent changes in reactant ratios and hence to obtain differential rates. At higher conversions, concentration gradients are present, i.e., reactant concentrations are not uniform across the chamber.[43] For all investigated mixtures herein, CO conversion exceeds 10% in the course of the heating ramp; for higher conversions, TOFs are affected to some extent by concentration gradients. TOFs up to conversions of 10% are indicated by black circles in Figure 3(b). For example, at 600 K TOFs of 420, 800, and 2100 CO_2 molecules $site^{-1}$ s^{-1} are reached for 2:1, 1:1, and 1:4 $CO:O_2$, which are well in the order of TOFs observed in the millibar regime by other groups.[16,26] Also at 0.1 mbar total pressure, the reaction is suffering from MTLs as deduced from Figure 3(d).

TABLE I. CO conversion in % for a 2:1 $CO:O_2$ mixture in an isothermal measurement; the XPS values in some cases are larger than the QMS values (see text); for the other studied gas mixtures a similar behavior was found.

CO/O_2	650 K	750 K	800 K	850 K	900 K
XPS (%)	5	43	53	60	60
QMS (%)	5	34	50	60	58

One point to be addressed is the fact that while the results derived from NAP-XPS and QMS measurements are in good qualitative agreement, they in some cases do show quantitative differences, that is, in some measurements we observed higher values for conversion by XPS than by the QMS analysis (see Figure 2 and Table I). A possible reason for this is the setup of our chamber. While XPS averages the gradients in gas phase concentrations between the sample and the analyser, the QMS detects the gas composition at the entrance to the differential pumping stages (see Figure 4) and therefore detects less CO_2 and correspondingly more CO. This difference depends on the exact sample position, which can reproduced only with certain accuracy.

As there is an on-going debate about the nature of the oxidation state of platinum in the most active regime, we also performed a temperature-programmed experiment in a highly oxidising $CO:O_2$ mixture of 1:10, at a total pressure p_{tot} = 1.1 mbar. For Pt(110), it was claimed that platinum oxide is the most reactive species under highly oxidising conditions, leading to a steep increase in CO_2 production at 425 K and 1 bar.[13,29] We chose a heating ramp of 2 K/min from 340 to 670 K; the respective online gas analysis of this experiment is shown in Figure 5. Note that the short increase in CO signal at the time of admission of O_2 to the chamber is attributed to desorption from the chamber walls. Above 450 K, a significant increase in CO_2 production occurs. This increase dramatically accelerates at 563 K: within 1 K (i.e., 8 data points), there is an abrupt jump of ~50% in CO_2 production (with 35% occurring within 4 s, i.e., 1 data point). Thereafter, the signal stays nearly constant (with a small decrease) until 600 K, and subsequently starts to decline significantly. Note that the expected corresponding pressure drop in the O_2 signal

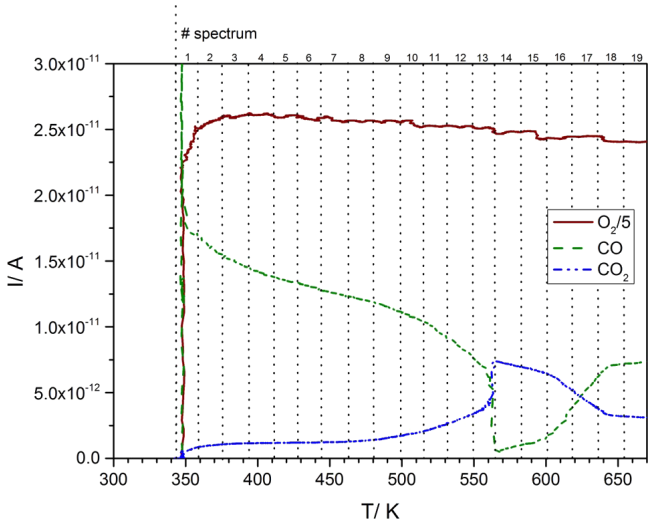

FIG. 5. Online gas analysis of a 1:10 CO:O_2 mixture with a heating ramp 300-670 K with ß = 2 K/min. Please note that the oxygen signal is divided by a factor of 5.

(m/z = 32) of only a few percent cannot be unequivocally discerned at the given noise level of the O_2 data in Figure 5.

We next take a close look at the O 1s XP spectra taken simultaneously, with a measuring time of 8 min/spectrum, i.e., a spectrum averages over a temperature range of ~17 K (the temperatures denoted in the following are the mean values); in Figure 6, selected spectra are shown and the denoted coverages were obtained from the total O 1s surface peak intensities. The spectra show the O 1s signals from the surface components,

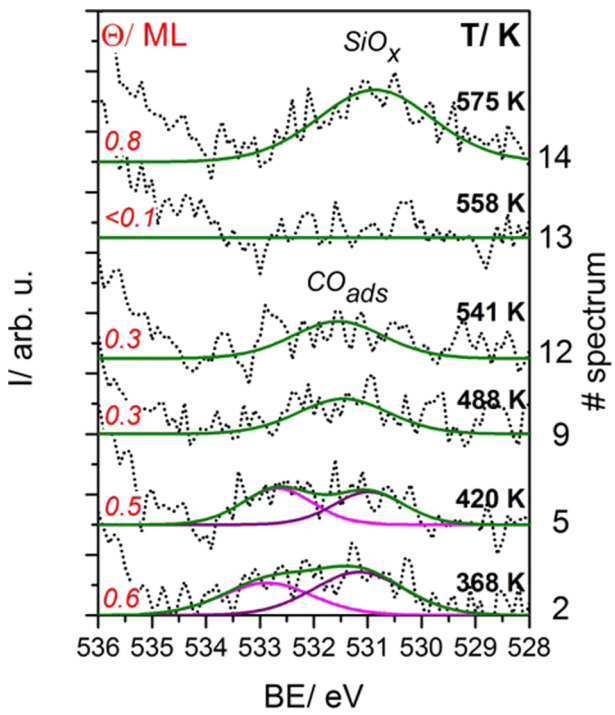

FIG. 6. Selected XP spectra of the O 1s region of the surface species during the experiment in Figure 5 for the 1:10 CO:O_2 mixture with a heating ramp 300-670 K with ß = 2 K/min; the surface coverages as determined from the total peaks areas are denoted. The temperatures of the XP spectra are given after half the spectrum was measured.

whereas the rise of signal intensity at the high binding energy side results from the gas phase signal.

For the lowest temperature, the O 1s signal of adsorbed CO is observed (~368 K; spectrum 2; CO bridge (purple) and on-top (pink) were fitted to guide the eye), which strongly decreases upon heating (~488 K; spectrum 9, and also ~541 K; spectrum 12); in the last spectrum before the abrupt jump in CO_2 production at 563 K, no oxygen-containing species is observed (558 K; spectrum 13). Only in the spectrum taken after the jump (575 K, spectrum 14), an oxygen signal is observed again, which is attributed to oxide formation. Interestingly, with the onset of this oxide formation, the CO_2 production rate starts to decrease, indicating that the formed oxide increasingly inhibits the reaction. The formed oxide is not a platinum oxide but is identified as silicon oxide (see below). No oxidation of the platinum is observed in the Pt 4f region taken after the measurement in UHV (see Figure S4 of the supplementary material).[36] At this point, we have to mention that although we do not see any O-containing species in the highly active regime, one has to keep in mind that a minority species with a coverage below our detection limit (here ~0.15 ML) could be responsible for the jump in activity at 563 K. In other words, we observe a jump from CO-covered to an adsorbate-"free"/clean surface—which could be the jump already observed in the literature when going from a carbon monoxide-covered to a oxygen-chemisorbed surface with a coverage below our detection limit.[26,42,44] In line with the interpretation of our *in situ* study that platinum oxide is not the active species, it was shown in an *ex situ* experiment that α-platinum oxide is far less reactive towards CO than chemisorbed oxygen.[45]

To summarize these results, we discussed the CO-inhibited regime at low temperatures and the role of the metallic, CO-free Pt surface (after CO desorption) as active phase with high activity for CO oxidation. Furthermore, we identified a third regime, where—in a very narrow temperature window—a dramatic increase of the CO_2 production occurs. It is likely that also in all other temperature-programmed experiments, this sudden change in reaction takes place, but due to the limited time/temperature resolution and diffusion effects, this effect is not sharp as observed signal increase in our online gas analysis.

B. Isothermal reaction

As a second method to examine the interaction of CO and O_2 with the Pt(111) surface, we performed isothermal measurements in order to gain information on the long term stability of the reaction. We again monitored the reaction simultaneously by NAP-XPS and QMS in a continuous flow mode.

We first exposed the surface to CO and after establishing a stable background pressure, oxygen was added to yield CO:O_2 ratios of 2:1 (stoichiometric), 1:1, and 1:4, with p_{tot} = 1 mbar. In all cases, the examination of the reaction over time did not show any significant changes of the activity during the isothermal experiments, which all took at least 3 h. As a representative example, the gas phase O 1s spectra of the stoichiometric 2:1 mixture at 750 K are shown in Figure 7

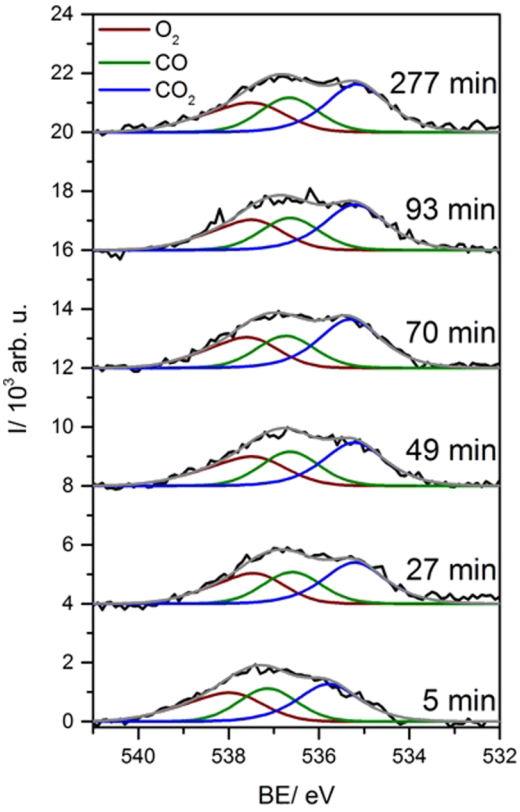

FIG. 7. *In situ* O 1s spectra of the gas phase of a 2:1 CO:O_2 mixture at 750 K and respective fits for O_2 (red), CO (green), CO_2 (blue), and envelope (dark green).

as a function of reaction time. They consist of three signals belonging to O_2, CO, and CO_2, whose ratios only change within the margin of error. Note that no O-containing surface species were detected during the reaction.

The reaction of CO to CO_2 is evident from the CO_2 peak in the O 1s spectra in Figure 7, but also from the QMS measurements (data not shown). Table I summarizes the quantitative XPS and QMS analysis for the stoichiometric 2:1 mixture. At 650 K, only negligible reaction occurred, while at 750 K, a significant reaction of CO is found (a conversion of 43% deduced from XPS data, and 34% from QMS; for an explanation of the larger value found in XPS, see Section III A). Upon further increasing the temperature to 850 K, even higher conversion is observed, which then levels off at higher temperatures (see Table I), due to mass transfer limitations.

As for the temperature-programmed experiments, the isothermal reaction depends on the oxygen percentage in the mixture. This is evident from Figure 8, where the TOFs for the different mixtures are plotted against reaction temperature, as derived from the O 1s NAP-XP spectra: for the 1:4 (CO:O_2) mixture, the reaction is very efficient already at 650 K, whereas for the stoichiometric (2:1) and for the slightly oxidising (1:1) gas compositions, only at 750 K significant reaction was observed. The observed trend is in line with literature,[40] where a lower onset in NAP-XP spectra was found at 535 K at a highly oxidising CO:O_2 ratio of 1:9, at a total pressure of 0.15 mbar. Again, no further increase in TOF is found from a certain temperature on, which is attributed to MTLs at the catalyst surface. The fact that MTLs start at lower

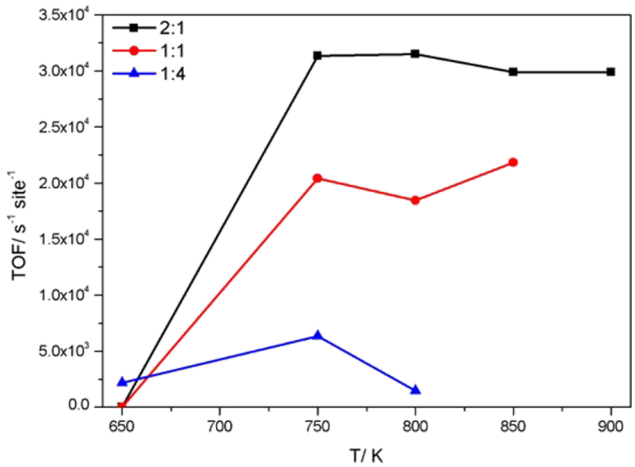

FIG. 8. TOFs vs reaction temperature for the isothermal reactions for the 2:1 (black), 1:1 (red), and 1:4 (blue) gas mixtures.

temperatures for the 1:4 mixture indicates that CO is the limiting reactant. The respective conversions are shown in Fig. S5 in the supplementary material.[36]

C. Growth and poisoning with "non-platinum"-oxides

In the course of our experiments, the development of an oxidic species at ~531.7 eV (slightly varying in binding energy) with time was detected in some of the O 1s region scans, especially at temperatures exceeding 600 K. A corresponding O 1s spectrum measured under UHV conditions after the growth of the respective oxide at 750 K is shown in Figure 9(a).

For some experiments, the growth of the oxide led to a decrease in CO_2 production up to total inhibition of the reaction within minutes (Figure 9(c)), as observed in XPS and QMS. The formed oxide is stable towards heating up to 1100 K in UHV and also in a CO atmosphere of 1 mbar at 800 K. This stability is not in line with observations for platinum oxides in the literature,[45] but has been observed for non-platinum oxides formed from minor bulk contamination of the Pt sample.[46–48]

Indeed, the survey spectrum (cf. Figure S6 of the supplementary material[36]) shows the emergence of the Si 2s signal characteristic of Si oxides with roughly Si:O_2 stoichiometry; a blow-up of the Si 2s signal from a different experiment is also shown in the inset of Figure 9(a). Note that the satellite of the Pt 4f signal overlaps with the Si 2p signals which are the strongest lines for silicon; therefore, only the weaker Si 2s signal is shown. The assignment is further supported by the absolute O 1s binding energy of 531.7 eV, which is typical for SiO_2, but much larger than the values of ~530 eV typically observed for platinum oxides.[33,45,49] Additionally, no changes were observed in the Pt 4f core level spectra taken before and after the oxidation experiment in UHV (see Figure 9(b)). The amount of silicon oxide increased with increasing oxygen partial pressure and/or temperature. By repeated oxidation/sputter cycles, the silicon impurities could be removed. Interestingly, exposing the sample to ambient conditions leads again to an increased amount of silicon in the near surface region.

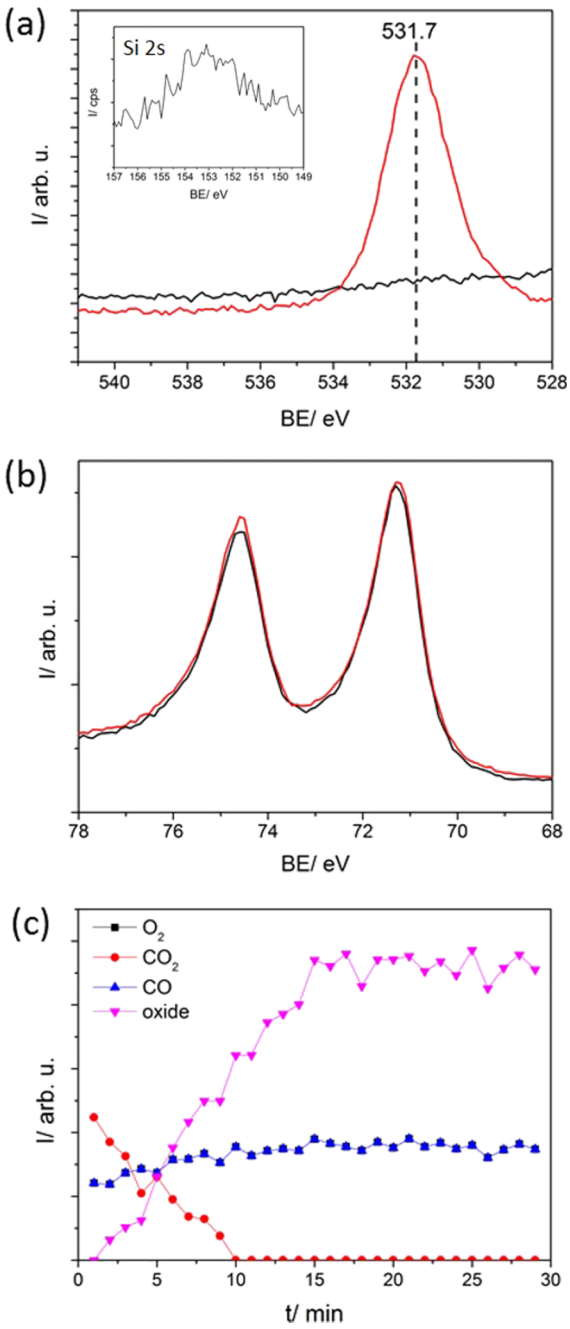

FIG. 9. (a) O 1s spectrum before reaction (black) and after pump-down in UHV (red) of the reaction for a 2:1 $CO:O_2$ mixture at 750 K and in the inset the Si 2s signal from the survey; (b) the respective Pt 4f core level spectra before reaction (black) and after pump-down of the reaction (red); and (c) integrated O 1s intensities (for the gas components O_2, CO, CO_2, and for surface oxide) vs time for the respective measurement.

IV. SUMMARY

In conclusion, we showed isothermal as well as temperature-programmed reaction experiments of the CO oxidation reaction for three different mixtures of $CO:O_2$ (2:1, 1:1, 1:4) at total pressures up to 1 mbar monitored by NAP-XPS and online gas analysis. The reaction was followed by XPS via the clearly separated O 1s gas phase signals of O_2, CO, and CO_2, and simultaneously by a QMS attached to the second differential pumping stage of the setup. With both techniques, the reaction was found to start at a certain onset temperature, which depends on the oxygen percentage of the mixture; the higher the relative oxygen content of the mixture, the lower the onset temperature. This behaviour is attributed to poisoning of the catalyst by CO and to a higher oxygen adsorption rate at higher oxygen content, due to the fact that adsorption of O_2 and (re-)adsorption of CO are competitive processes. At the investigated total pressures of 0.1 or 1 mbar for the different gas mixtures, the CO and O_2 partial pressures changed, influencing the ad- and desorption. The observations are in line with the literature, under the assumption of a Langmuir-Hinshelwood mechanism.[19] For both temperature-programmed and isothermal experiments, the highest TOFs were found for the stoichiometric mixtures. The TOFs increased with increasing temperature and stagnated at a particular temperature due to mass transfer limitations. While the results obtained from NAP-XPS and online gas analysis were qualitatively in good agreement, quantitative comparison showed that the QMS in some cases slightly underestimates the conversion, which is ascribed to different detection regions for the different methods. Concerning the reactive species in the active regime, we did not detect any oxygen-containing species on the surface in our temperature-programmed investigations and therefore, we conclude that no (or only a minor amount of) oxide is present and that the reactive surface is in a metallic state. Since the experiments were started out with a CO precovered catalyst surface, the reaction onset was determined by CO desorption. In an additional experiment using a highly oxidising mixture ($CO:O_2$ = 1:10; p_{tot} = 1.1 mbar) in combination with a considerably slower heating rate, three different regimes were observed: (I) CO-inhibited with negligible activity, (II) partially CO-covered with moderate activity, and (III) adsorbate-free with high activity. Upon prolonged heating, in some cases, the formation of SiO_2 was observed on the platinum surface; the growth of this oxide leads to a poisoning of the catalyst up to total inhibition of the reaction. This or similar "non-platinum" oxides result from minor Pt bulk impurities and hence similar effects should be considered also in heterogeneous catalysis.

ACKNOWLEDGMENTS

The financial support by the Cluster of Excellence "Engineering of Advanced Materials" and by the Alexander von Humboldt Foundation within the Research Group Linkage Programme is acknowledged.

[1]S. Hüfner, *Photoelectron Spectroscopy: Principles and Applications* (Springer, 2003).
[2]C. Papp and H.-P. Steinrück, Surf. Sci. Rep. **68**, 446 (2013).
[3]A. Baraldi, G. Comelli, S. Lizzit, M. Kiskinova, and G. Paolucci, Surf. Sci. Rep. **49**, 169 (2003).
[4]I. Niedermaier, N. Taccardi, P. Wasserscheid, F. Maier, and H.-P. Steinrück, Angew. Chem., Int. Ed. **52**, 8904 (2013).
[5]R. Denecke, Appl. Phys. A **88**, 977 (2005).
[6]A. Klein, T. Mayer, A. Thissen, and W. Jaegermann, Bunsen-Mag. **4**, 124 (2008).
[7]M. Salmeron and R. Schlögl, Surf. Sci. Rep. **63**, 169 (2008).
[8]H. Over, Y. D. Kim, A. P. Seitsonen, S. Wendt, E. Lundgren, M. Schmid, P. Varga, A. Morgante, and G. Ertl, Science **287**, 3 (2000).
[9]M. Bron, D. Teschner, A. Knopgericke, B. Steinhauer, A. Scheybal, M. Hävecker, D. Wang, R. Fodisch, D. Honicke, and A. Wootsch, J. Catal. **234**, 37 (2005).

[10]C. Stampfl, M. V. Ganduglia-Pirovano, K. Reuter, and M. Scheffler, Surf. Sci. **500**, 368 (2002).
[11]H. Bluhm, M. Hävecker, A. Knop-Gericke, M. Kiskinova, R. Schlögl, and M. Salmeron, MRS Bull. **32**, 1022 (2007).
[12]D. E. Starr, Z. Liu, M. Hävecker, A. Knop-Gericke, and H. Bluhm, Chem. Soc. Rev. **42**, 5833 (2013).
[13]B. L. M. Hendriksen, S. C. Bobaru, and J. W. M. Frenken, Top. Catal. **36**, 43 (2005).
[14]S. Matera and K. Reuter, Catal. Lett. **133**, 156 (2009).
[15]S. Blomberg, M. Hoffmann, J. Gustafson, N. Martin, V. Fernandes, A. Borg, Z. Liu, R. Chang, S. Matera, K. Reuter, and E. Lundgren, Phys. Rev. Lett. **110**, 117601 (2013).
[16]A. Farkas, K. Zalewska-Wierzbicka, C. Bachmann, J. Goritzka, D. Langsdorf, O. Balmes, J. Janek, and H. Over, J. Phys. Chem. C **117**, 9932 (2013).
[17]R. L. Palmer, J. Chem. Phys. **60**, 1453 (1974).
[18]I. Langmuir, J. Chem. Soc., Faraday Trans. **17**, 607 (1922).
[19]C. T. Campbell, G. Ertl, H. Kuipers, and J. Segner, J. Chem. Phys. **73**, 5862 (1980).
[20]M. Kinne, T. Fuhrmann, J. F. Zhu, C. M. Whelan, R. Denecke, and H.-P. Steinrück, J. Chem. Phys. **120**, 7113 (2004).
[21]G. Ertl, Angew. Chem., Int. Ed. **47**, 3524 (2008).
[22]G. Ertl, Science **254**, 6 (1991).
[23]G. Ertl, P. Norton, and J. Rüstig, Phys. Rev. Lett. **49**, 177 (1982).
[24]M. P. Cox, G. Ertl, R. Imbihl, and J. Rüstig, Surf. Sci. **134**, L517 (1983).
[25]R. C. Yeates, J. E. Turner, A. J. Gellman, and G. A. Somorjai, Surf. Sci. **149**, 175 (1985).
[26]F. Gao, Y. Wang, Y. Cai, and D. W. Goodman, J. Phys. Chem. C **113**, 174 (2009).
[27]F. Gao, Y. Wang, and D. W. Goodman, J. Phys. Chem. C **114**, 6874 (2010).
[28]R. van Rijn, O. Balmes, R. Felici, J. Gustafson, D. Wermeille, R. Westerström, E. Lundgren, and J. W. M. Frenken, J. Phys. Chem. B **114**, 6875 (2010).
[29]B. L. M. Hendriksen and J. W. M. Frenken, Phys. Rev. Lett. **89**, 46101 (2002).
[30]M. Ackermann, T. Pedersen, B. L. M. Hendriksen, O. Robach, S. C. Bobaru, I. Popa, C. Quiros, H. Kim, B. Hammer, S. Ferrer, and J. W. M. Frenken, Phys. Rev. Lett. **95**, 255505 (2005).
[31]X. Su, P. S. Cremer, Y. R. Shen, and G. A. Somorjai, J. Am. Chem. Soc. **119**, 3994 (1997).
[32]C. Ellinger, A. Stierle, I. K. Robinson, A. Nefedov, and H. Dosch, J. Phys.: Condens. Matter **20**, 184013 (2008).
[33]D. J. Miller, H. Öberg, S. Kaya, H. Sanchez Sasalongue, D. Friebel, T. Anniyev, H. Ogasawara, H. Bluhm, L. G. M. Pettersson, and A. Nilsson, Phys. Rev. Lett. **107**, 195502 (2011).
[34]J. Pantförder, S. Pöllmann, J. F. Zhu, D. Borgmann, R. Denecke, and H.-P. Steinrück, Rev. Sci. Instrum. **76**, 14102 (2005).
[35]M. Kinne, T. Fuhrmann, C. M. Whelan, J. F. Zhu, J. Pantförder, M. Probst, G. Held, R. Denecke, and H.-P. Steinrück, J. Chem. Phys. **117**, 10852 (2002).
[36]See supplementary material at http://dx.doi.org/10.1063/1.4940318 for details on the fitting procedure and additional measurements.
[37]G. Ertl, M. Neumann, and K. M. Streit, Surf. Sci. **64**, 393 (1977).
[38]F. Gao, Y. Cai, K. K. Gath, Y. Wang, M. S. Chen, Q. L. Guo, and D. W. Goodman, J. Phys. Chem. C **113**, 182 (2009).
[39]M. Kinne, T. Fuhrmann, J. F. Zhu, B. Tränkenschuh, R. Denecke, and H.-P. Steinrück, Langmuir **20**, 7 (2004).
[40]J. Schnadt, J. Knudsen, J. N. Andersen, H. Siegbahn, A. Pietzsch, F. Hennies, N. Johansson, N. Martensson, G. Ohrwall, S. Bahr, S. Mahl, and O. Schaff, J. Synchrotron Radiat. **19**, 701 (2012).
[41]J. Zetterberg, S. Blomberg, J. Gustafson, Z. W. Sun, Z. S. Li, E. Lundgren, and M. Alden, Rev. Sci. Instrum. **83**, 53104 (2012).
[42]M. S. Chen, Y. Cai, Z. Yan, K. K. Gath, S. Axnanda, and D. W. Goodman, Surf. Sci. **601**, 5326 (2007).
[43]P. Harriott, *Chemical Reactor Design* (Marcel Denker, Inc, 2003).
[44]F. Gao, S. McClure, M. Chen, and D. W. Goodman, J. Phys. Chem. C **114**, 22369 (2010).
[45]D. J. Miller, H. Sanchez Casalongue, H. Bluhm, H. Ogasawara, A. Nilsson, and S. Kaya, J. Am. Chem. Soc. **136**, 6340 (2014).
[46]H. Niehus and G. Comsa, Surf. Sci. **102**, L14 (1981).
[47]M. Salmeron, L. Brewer, and G. A. Somorjai, Surf. Sci. **112**, 207 (1981).
[48]H. P. Bonzel, A. M. Franken, and G. Pirug, Surf. Sci. **104**, 625 (1981).
[49]T. C. Rocha, A. Oestereich, D. V. Demidov, M. Hävecker, S. Zafeiratos, G. Weinberg, V. I. Bukhtiyarov, A. Knop-Gericke, and R. Schlögl, Phys. Chem. Chem. Phys. **14**, 4554 (2012).